We are IntechOpen,
the world's leading publisher of
Open Access books
Built by scientists, for scientists

4,800
Open access books available

122,000
International authors and editors

135M
Downloads

Our authors are among the

154
Countries delivered to

TOP 1%
most cited scientists

12.2%
Contributors from top 500 universities

BOOK CITATION INDEX
CLARIVATE ANALYTICS
INDEXED

WEB OF SCIENCE™

Selection of our books indexed in the Book Citation Index
in Web of Science™ Core Collection (BKCI)

Interested in publishing with us?
Contact book.department@intechopen.com

Numbers displayed above are based on latest data collected.
For more information visit www.intechopen.com

Gust Alleviation Control Using Robust MPC

Masayuki Sato[1], Nobuhiro Yokoyama[2] and Atsushi Satoh[3]
[1]Japan Aerospace Exploration Agency
[2]National Defense Academy
[3]Iwate University
Japan

1. Introduction

Disturbance suppression is one of the very important objectives for controller design. Thus, many papers on this topic have been reported, e.g. (Xie & de Souza, 1992; Xie et al., 1992). This kind of problem can be described as an H_∞ controller design problem using a fictitious performance block (Zhou et al., 1996). Therefore, disturbance suppression controllers can be easily designed by applying the standard H_∞ controller design method (Fujita et al., 1993).

Disturbance suppression is also important in aircraft motions (*Military Specification: Flight Control Systems - Design, Installation and Test of Piloted Aircraft, General Specification For*, 1975), and the design problem of flight controllers which suppress aircraft motions driven by wind gust, i.e. Gust Alleviation (GA) flight controller design problem (in short GA problem), has been addressed (Botez et al., 2001; Hess, 1971; 1972). In those papers, only the state information related to aircraft motions (such as, pitch angle, airspeed, etc.) is exploited for the control of aircraft motions. However, if turbulence information is obtained *a priori* and can also be exploited for the control, it is inferred that GA performance will be improved. This idea has already been adopted by several researchers (Abdelmoula, 1999; Phillips, 1971; Rynaski, 1979a;b; Santo & Paim, 2008).

Roughly speaking, GA problem is to design flight controllers which suppress the vertical acceleration driven by turbulence. In the 1970s, turbulence was measured at the nose of aircraft (Phillips, 1971); however, the lead time from the measurement of turbulence to its acting on aircraft motions becomes very short as aircraft speed increases. Thus, the turbulence data which were measured at the nose of aircraft could not be effectively used. On this issue, as electronic and optic technologies have advanced in the last two decades, nowadays, turbulence can be measured several seconds ahead using LIght Detection And Ranging (LIDAR) system (Ando et al., 2008; Inokuchi et al., 2009; Jenaro et al., 2007; Schmitt et al., 2007). This consequently means that GA control exploiting turbulence data which are measured *a priori* now becomes more practical than before. Thus, this paper addresses the design problem of such GA flight controllers.

If disturbance data are supposed to be given *a priori* and the current state of plant is also available, then controllers using Model Predictive Control (MPC) scheme work well, as illustrated for active suspension control for automobiles (Mehra et al., 1997; Tomizuka, 1976). However, in those papers, it is supposed that the plant dynamics are exactly modeled; that is, robustness of controllers against the plant uncertainties (such as, modeling errors, neglected

nonlinearities, etc.) is not considered. From a practical standpoint, it is very difficult to obtain the exact plant model. If controllers are designed without the consideration of plant uncertainties then the controlled system might achieve very poor control performance, or even worse the controlled system might be unstable. Thus, it is very important to ensure the robustness of controllers against plant uncertainties.

There have been a lot of papers which propose the design methods of MPC ensuring robustness against plant uncertainties, e.g. (Badgwell, 1997; Bemporad & Morari, 1999; Kothare et al., 1996; Kwon & Han, 2005; Löfberg, 2003; Takaba, 2000). Generally speaking, MPC design for uncertain plant leads to a design problem with infinitely many conditions. However, it is intrinsically very hard to solve this kind of problems. In the above papers, the difficulty of solving infinitely many conditions is successfully circumvented by introducing some conservatism. For example, the controllers are designed by solving Linear Matrix Inequalities (LMIs) associated with H_∞ performance or H_2 performance using common Lyapunov functions (Kothare et al., 1996; Takaba, 2000), or invariant ellipsoids being encompassed by the original invariant sets are used to ensure robust performance (Löfberg, 2003). Common Lyapunov functions as well as invariant ellipsoids generally introduce conservatism, which should be reduced.

The plant model for real systems usually includes various types of uncertainties, e.g. parametric uncertainties, neglected nonlinearities, uncertain dead time, etc. If the operating range of aircraft is relatively small and the nominal aircraft motion model is well known, then the uncertainty to be considered most is the unmodeled dynamics, which usually lie in high frequency range. One of the effective representations of this kind of uncertainties is bounded uncertain delays at the control input channels (Miyazawa, 1995; Ohno et al., 1999; Sato & Satoh, 2008), in which the effectiveness of this model is demonstrated with applications to real aircraft. Since the delay at the control input generally augments phase lag in the high frequency range, the controller designed using this type of uncertainty would have sufficiently large stability margin in the high frequency range. Therefore, this paper supposes that plant uncertainties are expressed as bounded time-invariant uncertain delays at the control input channels.

In this paper, turbulence is supposed to be measured *a priori*. The measured data always have measurement errors, such as, calibration error, position error, etc. Therefore, when exploiting the measured turbulence data for controller design, the measurement errors should be considered.

Considering these backgrounds, this paper addresses the following controller design problem: GA flight controllers exploiting *a priori* measured turbulence data including some measurement errors for aircraft motions with bounded time-invariant uncertain delays at the control input. We show that this problem is reduced to a robust MPC with finitely many conditions with neither conservatism nor approximations being introduced. The proposed MPC is formulated in terms of a Second-Order Cone Programming (SOCP) problem (Boyd & Vandenberghe, 2004), which is easily solved by using some of the generally available software, e.g. (Sturm, 1999).

Hereafter, 0_n, $0_{n,m}$, $\mathbf{0}$ and I_n respectively denote an $n \times n$ dimensional zero matrix, an $n \times m$ dimensional zero matrix, an appropriately dimensioned zero matrix and an $n \times n$ dimensional identity matrix, $\mathbf{1}_n$ denotes an n-dimensional vector with all elements being unities, $\mathcal{Z}$, $\mathcal{R}^n$ and $\mathcal{R}^{n \times m}$ respectively denote the set of integers, the set of n-dimensional real vectors and the set of $n \times m$ dimensional real matrices, $\otimes$ denotes Kronecker product, and $\lceil p \rceil$ denotes

$\min \{n \in \mathcal{Z} | p \leq n\}$. For n-dimensional vectors $p = [p_1 \; \cdots \; p_n]^T$ and $r = [r_1 \; \cdots \; r_n]^T$, $p \leq r$ denotes that $p_i \leq r_i$ holds for all i, that is, the inequality holds element-wise.

2. Preliminaries

In this section, the supposed aircraft motion model with uncertain delays at the control input is first defined and a family of models representing the aircraft motions is derived, then *a priori* measured turbulence data with some measurement errors are defined, and finally the addressed problem is given.

2.1 Uncertain plant system

Let us define the nominal continuous-time linearized aircraft motion model including actuator dynamics as P_c.

$$P_c : \begin{cases} \dot{x}(t) = A_c x(t) + B_{1_c} w(t) + B_{2_c} u(t) \\ z(t) = C_c x(t) + D_{1_c} w(t) + D_{2_c} u(t) \end{cases}, \tag{1}$$

where $x(t) \in \mathcal{R}^n$, $w(t) \in \mathcal{R}^{n_w}$, $u(t) \in \mathcal{R}^{n_u}$, and $z(t) \in \mathcal{R}^{n_z}$ respectively denote the state which includes the variables related to the aircraft motions (e.g. velocity, pitch angle, etc.) and the variables related to the control actuators, the turbulence input, the control input (e.g. elevator command), and the performance output which characterizes the motion to be suppressed (e.g. vertical acceleration). All states are supposed to be measurable and available.

The uncertainties of the plant are supposed to be represented as delays with bounded time-invariant uncertain delay time at the control input. Thus, the control input $u(t)$ is given as

$$u(t) = v(t - T_d), \tag{2}$$

where $v(t) \in \mathcal{R}^{n_u}$ denotes the control input command created by the onboard flight computer and T_d [s] denotes the uncertain delay time which is assumed to lie in the interval between $T_{d_{\min}}$ and $T_{d_{\max}}$.

$$T_d \in \left[T_{d_{\min}}, \; T_{d_{\max}} \right] \tag{3}$$

Considering the delay due to the calculation of the control input command with the onboard computer, the minimum delay time $T_{d_{\min}}$ is assumed to be larger than or equal to the sampling period of the onboard computer which is given as T_s [s].

$$T_s \leq T_{d_{\min}} \tag{4}$$

Similarly to usual MPC in the literature (Bemporad & Morari, 1999; Kothare et al., 1996; Löfberg, 2003), the discretized plant of P_c is considered for controller design. Suppose that the discretized plant of P_c is given as P_d using a zero-order hold which is a common method for the discretization.

$$P_d : \begin{cases} x_{k+1} = A x_k + B_1 w_k + B_2 u_k \\ z_k = C x_k + D_1 w_k + D_2 u_k \end{cases}, \tag{5}$$

where $x_k \in \mathcal{R}^n$, $w_k \in \mathcal{R}^{n_w}$, $u_k \in \mathcal{R}^{n_u}$, and $z_k \in \mathcal{R}^{n_z}$ respectively denote the state, the turbulence, the control input, and the performance output of P_d at step k. The sampling period for the discretization is assumed to be the same as that of the onboard computer T_s [s]. As all states of P_c are supposed to be measurable and available, all states of P_d are also supposed to be measurable and available.
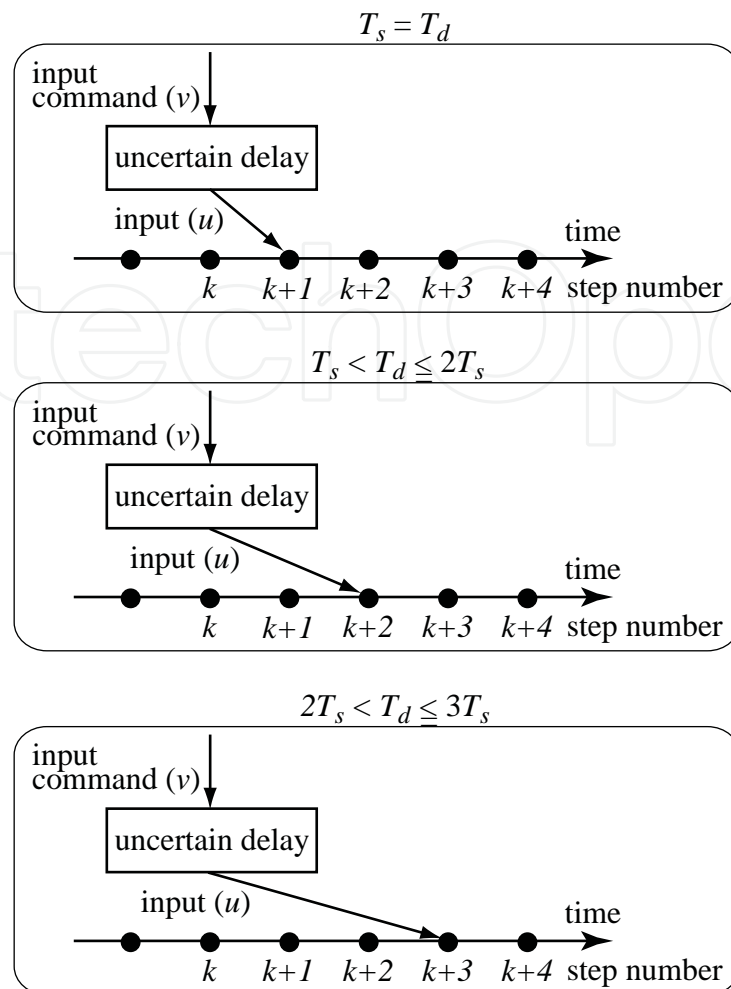
Fig. 1. Effect of uncertain delay

Remark 1. *In equation (5), the turbulence w_k is supposed be constant during the sampling period T_s. Strictly speaking, this does not hold true. However, if the sampling period is sufficiently small compared to the period corresponding to the typical frequency of turbulence then the turbulence can be regarded as constant during the sampling period.*

Similarly, the delay system (2) must be discretized. As the control input is applied not continuously but discretely, the delay effect of the control input command to the actual control input appears only at the sampling steps. That is, in a sharp contrast to a continuous-time case, in a discrete-time case, the whole elements of delay step set $\mathcal{T}_d$, which is defined as (6), are only to be considered as the uncertain delay T_d lying in the interval $\left[T_{d_{\min}}, \ T_{d_{\max}} \right]$.

$$\mathcal{T}_d = \left\{ \underline{d}, \underline{d} + 1, \cdots, \overline{d} \right\}, \tag{6}$$

where $\underline{d}$ and $\overline{d}$ are respectively defined as $\left\lceil \frac{T_{d_{\min}}}{T_s} \right\rceil$ and $\left\lceil \frac{T_{d_{\max}}}{T_s} \right\rceil$ (see Fig. 1). The number of the elements in set $\mathcal{T}_d$ is denoted by $\hat{d}(= \overline{d} - \underline{d} + 1)$. Thus, the delay steps belonging to set T_d are only to be considered in the discrete-time systems, while all possible delays lying in $\left[T_{d_{\min}}, \ T_{d_{\max}} \right]$ must be considered in the continuous-time systems. Then, the control input u_k is given as one of the elements of the following set:

$$\left\{ v_{k-\underline{d}}, v_{k-\underline{d}-1}, \cdots, v_{k-\overline{d}} \right\}, \tag{7}$$

where v_m denotes the control input command of P_d created at step m; however, the real input u_k which is applied to P_d is unknown.

Now, the control input command v_k is factorized into the previous control input command v_{k-1} and the deviation between these commands to consider the rate limit of the control input command, i.e.

$$v_k = v_{k-1} + \Delta v_k, \tag{8}$$

where the previous control input command at step 0, v_{-1}, is set $\mathbf{0}$.

Under these preliminaries, the supposed plant P_u, which is composed of P_d and the uncertain delays at the control input, is described as follows.

$$P_u \in \left\{ P_u^{\underline{d}}, P_u^{\underline{d}+1}, \cdots, P_u^{\overline{d}} \right\}, \tag{9}$$

where P_u^i $(i = \underline{d}, \underline{d} + 1, \cdots, \overline{d})$ is defined as

$$P_u^i : \begin{cases} \hat{x}_{k+1}^i = \hat{A}^i \hat{x}_k^i + \hat{B}_1^i w_k + \hat{B}_2^i \Delta v_k \\ z_k^i = \hat{C}^i \hat{x}_k^i + \hat{D}_1^i w_k + \hat{D}_2^i \Delta v_k \end{cases}, \tag{10}$$

where $\hat{x}_k^i$ denotes the augmented state of i-th plant model at step k and is defined as $\hat{x}_k^i := \begin{bmatrix} x_k^{i\,T} & v_{k-\overline{d}}^T & \cdots & v_{k-1}^T \end{bmatrix}^T$ with x_k^i which denotes the state of i-th plant model at step k. The matrices $\hat{A}^i$, etc. are defined in (11).

$$\left[\begin{array}{c|c|c} \hat{A}^i & \hat{B}_1^i & \hat{B}_2^i \\ \hline \hat{C}^i & \hat{D}_1^i & \hat{D}_2^i \end{array} \right]$$

$$:= \begin{cases} \left[\begin{array}{ccc|c|c} A & 0_{n,n_u(\overline{d}-1)} & B_2 & B_1 & 0_{n,n_u} \\ 0_{n_u(\overline{d}-1),n} & 0_{n_u(\overline{d}-1),n_u(\overline{d}-1)} & 0_{n_u(\overline{d}-1),n_u} & 0_{n_u(\overline{d}-1),n_w} & 0_{n_u(\overline{d}-1),n_u} \\ 0_{n_u,n} & 0_{n_u,n_u(\overline{d}-1)} & 0_{n_u,n_u} & 0_{n_u,n_w} & I_{n_u} \\ \hline C & 0_{n_z,n_u(\overline{d}-1)} & 0_{n_z,n_u} & D_1 & D_2 \end{array} \right] \quad (i = 1) \\[2em] \left[\begin{array}{ccc|c} A & 0_{n,n_u(\overline{d}-i)} & B_2 & 0_{n,n_u(i-1)} \\ 0_{n_u(\overline{d}-1),n} & 0_{n_u(\overline{d}-1),n_u(\overline{d}-i)} & 0_{n_u(\overline{d}-1),n_u} & \begin{bmatrix} 0_{n_u(\overline{d}-i),n_u(i-1)} \\ I_{n_u(i-1)} \end{bmatrix} \\ 0_{n_u,n} & 0_{n_u,n_u(\overline{d}-i)} & 0_{n_u,n_u} & \begin{bmatrix} 0_{n_u,n_u(i-2)} & I_{n_u} \end{bmatrix} \\ \hline C & 0_{n_z,n_u(\overline{d}-i)} & 0_{n_z,n_u} & \begin{bmatrix} 0_{n_z,n_u(i-2)} & D_2 \end{bmatrix} \end{array} \right. \\ \qquad \left. \begin{array}{c|c} & B_1 & 0_{n,n_u} \\ & 0_{n_u(\overline{d}-1),n_w} & 0_{n_u(\overline{d}-1),n_u} \\ & 0_{n_u,n_w} & I_{n_u} \\ \hline & D_1 & D_2 \end{array} \right] \quad (i \neq 1) \end{cases} \tag{11}$$

Remark 2. *Although the uncertainty model using the delay (2) with bounded time-invariant uncertain delay (3) generally introduces some approximations from the real uncertainties of aircraft motions, the derivation of a family of plant models (9) from the supposed uncertainties, i.e. the delay (2),*

introduces neither assumptions nor approximations. Thus, the formulation above introduces no further conservatism from the supposed uncertain plant model.

Remark 3. *It is stressed that matrices $\hat{A}^i$, etc. in (11) have no uncertainties.*

As the current state x_k of P_d is supposed to be available, and previously created control input commands, $v_{k-\overline{d}}, \cdots, v_{k-1}$, can be memorized in the onboard computer which produces the control input command, the augmented state of i-th plant model, $\hat{x}_k^i$, is supposed to be available and given as $\hat{x}_k$. Then, the following holds.

$$\hat{x}_k = \hat{x}_k^{\underline{d}} = \hat{x}_k^{\underline{d}+1} = \cdots = \hat{x}_k^{\overline{d}} \tag{12}$$

Hereafter, the plant model for designing controllers for P_c with $u(t)$ being given as (2) is P_u.

2.2 Uncertain turbulence data

Using some system, such as, LIDAR system, it is supposed that turbulence w is measured before the turbulence affects the aircraft motions. Generally speaking, the measured data have measurement errors even if the calibration was conducted before its use. Thus, it is supposed that the j step ahead real turbulence at step k, which is denoted by w_{k+j}, satisfies the following relation with the j step ahead turbulence that is measured at step k, which is denoted by $w_{k+j|k}$.

$$\tilde{w} := \begin{bmatrix} w_k \\ w_{k+1} \\ \vdots \\ w_{k+N-1} \end{bmatrix} = \begin{bmatrix} w_{k|k} \\ w_{k+1|k} \\ \vdots \\ w_{k+N-1|k} \end{bmatrix} + \begin{bmatrix} X_0 \\ X_1 \\ \vdots \\ X_{N-1} \end{bmatrix} \Delta_w, \tag{13}$$

where N, which is given as a constant positive integer, denotes the maximum step number for measuring turbulence *a priori*, $X_j \in \mathcal{R}^{n_w \times n_w}$ $(j = 0, 1, \cdots, N-1)$ denote the constant given matrices which define the measurement errors in the measured turbulence data with uncertain constant vector $\Delta_w \in \mathcal{R}^{n_w}$ satisfying (14) (see Fig. 2, which is at the top of the next page).

$$-\mathbf{1}_{n_w} \leq \Delta_w \leq \mathbf{1}_{n_w} \tag{14}$$

Let us define set Ω as the existence region of $\tilde{w}$.

$$\Omega = \left\{ \tilde{w} \in \mathcal{R}^{n_w N} : \tilde{w} \text{ given as (13) with } \Delta_w \text{ satisfying (14)} \right\} \tag{15}$$

Remark 4. *Note that matrices X_j might be different for each j; that is, it is possible that $X_0 \neq X_1 \neq \cdots \cdots \neq X_{N-1}$ holds. Furthermore, note that matrices X_j might be different for each step k; that is, matrices $X_0, \cdots, X_{N-1}$ at step k might be different from the corresponding matrices $X_0, \cdots, X_{N-1}$ at step $k-1$. This corresponds to time-varying measurement error case.*

Remark 5. *Note that $\tilde{w}$ is affine with respect to the each element of Δ_w.*

Hereafter, it is supposed that at each step the real turbulence data w_{k+j} are not available *a priori*, but instead, the measured data $w_{k+j|k}$ which satisfy (13) with measurement errors defined as $X_j \Delta_w$ are available.
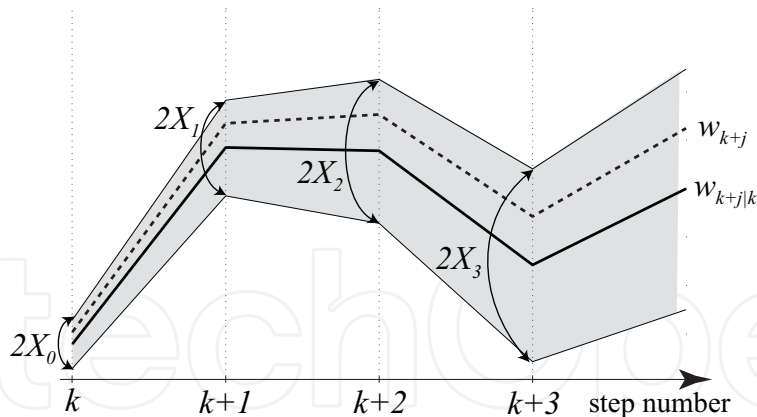
Fig. 2. Measurement error at step k in case for $n_w = 1$ and $X_j(\in \mathcal{R}) > 0$

2.3 Problem definition

Using the uncertain plant model P_u given as (9) using (10) and the *a priori* measured turbulence data $w_{k+j|k}$ satisfying (13), the addressed problem, i.e. GA problem exploiting the *a priori* measured turbulence data, is defined below.

Considering that the turbulence are measured for N steps ahead, the horizon step number in MPC, which denotes the step number during which control performance is to be optimized, is also set N. For i-th plant model P_u^i, the performance index for turbulence suppression, i.e. GA performance, is defined as

$$J_i(\hat{x}^i, \Delta v, z^i) = \sum_{j=0}^{N-1} \left((\hat{x}^i_{k+j+1|k})^T Q \hat{x}^i_{k+j+1|k} + \Delta v^T_{k+j|k} R \Delta v_{k+j|k} + (z^i_{k+j|k})^T S z^i_{k+j|k} \right), \quad (16)$$

where matrices Q and S are appropriately defined positive semidefinite matrices, matrix R is an appropriately defined positive definite matrix, $\hat{x}^i_{k+j|k}$ denotes the i-th plant's augmented state at step $k + j$ predicted at step k, $\Delta v_{k+j|k}$ denotes the control input command deviation at step $k + j$ created at step k, and $z^i_{k+j|k}$ denotes the performance output at step $k + j$ predicted at step k.

There usually exist preferable or prohibitive regions for the state, the performance output, and the control input command deviation. For the consideration of these regions, constraints for the augmented state $\hat{x}^i$, the control input command deviation Δv and the performance output z^i are introduced. That is, they should satisfy the following constraints.

$$\gamma_{\min} \le \hat{x}^i_{k+j+1|k} \le \gamma_{\max}, \; j = 0, \cdots, N-1, \quad (17)$$

$$\delta_{\min} \le \Delta v_{k+j|k} \le \delta_{\max}, \; j = 0, \cdots, N-1, \quad (18)$$

$$\xi_{\min} \le z^i_{k+j|k} \le \xi_{\max}, \; j = 0, \cdots, N-1, \quad (19)$$

where $\gamma_{\min}, \gamma_{\max} \in \mathcal{R}^{n+n_u\bar{d}}$, $\delta_{\min}, \delta_{\max} \in \mathcal{R}^{n_u}$ and $\xi_{\min}, \xi_{\max} \in \mathcal{R}^{n_z}$ are given constant vectors.

If the worst performance of $J_i(\hat{x}^i, \Delta v, z^i)$ $(i = \underline{d}, \cdots, \overline{d})$ is minimized then all the other performance of $J_i(\hat{x}^i, \Delta v, z^i)$ is no more than the worst; that is, all the possible plant models P_u^i have no more worse performance than the worst. Considering this, the design objective is to

obtain $\Delta v_{k+j|k}$ which minimizes the maximum of $J_i(\hat{x}^i, \Delta v, z^i)$. Thus, the addressed problem is defined as follows.

Problem 1. *Suppose that uncertain aircraft motion model is given as P_u defined as in (9) using P_u^i in (10), that the current augmented state $\hat{x}_k$ is available, and that j ($j = 0, \cdots, N - 1$) step ahead turbulence at step k is measured as $w_{k+j|k}$ which satisfies (13) for the real turbulence w_{k+j}.*
Under these assumptions, find $\Delta v_{k+j|k}$ ($j = 0, \cdots, N - 1$) which minimize
$\max\limits_{\tilde{w}\in\Omega} \max\limits_{i\in\{\underline{d},\cdots,\overline{d}\}} J_i(\hat{x}^i, \Delta v, z^i)$ *under the constraints (17), (18) and (19).*

If Problem 1 is solved online, then the control input command v at step k, v_k, is calculated as $v_{k-1} + \Delta v_{k|k}$ using the previous control input command v_{k-1}. The control strategy of this paper is to obtain the optimal control input command by solving an optimization problem online using a family of plant models. That is, the proposed control strategy is MPC.
It is easily confirmed that solving Problem 1 is equivalent to solving the following problem.

Problem 2. *Find $\Delta v_{k+j|k}$ ($j = 0, \cdots, N - 1$) which minimize the following performance index.*

$$\max\limits_{\tilde{w}\in\Omega} \max\limits_{i\in\{\underline{d},\cdots,\overline{d}\}} J_i(\hat{x}^i, \Delta v, z^i) \text{ subject to } (17), (18), (19), (10) \text{ with } (12) \text{ and } (13)$$

Remark 6. *Note that Problem 2 seeks the common control input command deviation for all i and for all possible $\tilde{w} \in \Omega$. Therefore, solving Problem 2 produces control input command deviation $\Delta v_{k|k}$ which is robust against the uncertain delays at the control input satisfying (3) and all possible turbulence $\tilde{w} \in \Omega$.*

In the next section, the proposed method to solve Problem 2 is shown.

3. Proposed method

In this section, the proposed method to solve Problem 2 is shown. For simplicity, let us first consider the case in which the measured turbulence data have no measurement errors, i.e. $w_{k+j} = w_{k+j|k}$, next consider the case in which the measured turbulence data have the measurement errors.

3.1 No measurement error case
Let all X_j in (13) be set as $\mathbf{0}$. Then, w_{k+j} is given as $w_{k+j|k}$. That is, the following holds.

$$\tilde{w} = \begin{bmatrix} w_{k|k}^T & \cdots & w_{k+N-1|k}^T \end{bmatrix}^T$$

Define the following vectors.

$$\tilde{v} = \begin{bmatrix} \Delta v_{k|k}^T & \cdots & \Delta v_{k+N-1|k}^T \end{bmatrix}^T$$
$$\tilde{x}^i = \begin{bmatrix} (\hat{x}_{k+1|k}^i)^T & \cdots & (\hat{x}_{k+N|k}^i)^T \end{bmatrix}^T, i = \underline{d}, \cdots, \overline{d}$$
$$\tilde{z}^i = \begin{bmatrix} (z_{k|k}^i)^T & \cdots & (z_{k+N-1|k}^i)^T \end{bmatrix}^T, i = \underline{d}, \cdots, \overline{d}$$

Then, the state equation and the performance output equation of P_u^i are respectively given as follows:

$$\tilde{x}^i = \left[I_N \otimes \hat{A}^i \ 0_{(n+n_u\overline{d})N, n+n_u\overline{d}} \right] \begin{bmatrix} \hat{x}_{k|k}^i \\ \tilde{x}^i \end{bmatrix} + \left(I_N \otimes \hat{B}_1^i \right) \tilde{w} + \left(I_N \otimes \hat{B}_2^i \right) \tilde{v}, \tag{20}$$

$$\tilde{z}^i = \left[I_N \otimes \hat{C}^i \ 0_{n_z N, n+n_u\overline{d}} \right] \begin{bmatrix} \hat{x}_{k|k}^i \\ \tilde{x}^i \end{bmatrix} + \left(I_N \otimes \hat{D}_1^i \right) \tilde{w} + \left(I_N \otimes \hat{D}_2^i \right) \tilde{v}. \tag{21}$$

Define the following matrices and vectors:

$$\tilde{Q} := I_N \otimes Q, \ \tilde{R} := I_N \otimes R, \ \tilde{S} := I_N \otimes S,$$

$$\tilde{\gamma}_{\min} := \mathbf{1}_N \otimes \gamma_{\min}, \ \tilde{\gamma}_{\max} := \mathbf{1}_N \otimes \gamma_{\max},$$
$$\tilde{\delta}_{\min} := \mathbf{1}_N \otimes \delta_{\min}, \ \tilde{\delta}_{\max} := \mathbf{1}_N \otimes \delta_{\max},$$
$$\tilde{\xi}_{\min} := \mathbf{1}_N \otimes \xi_{\min}, \ \tilde{\xi}_{\max} := \mathbf{1}_N \otimes \xi_{\max}.$$

Using these definitions, the following proposition, which is equivalent to Problem 2, is directly obtained.

Proposition 1. *Find $\tilde{v}$ which minimizes q subject to (22), (23), and (24).*

$$q \geq \begin{bmatrix} \tilde{x}^i \\ \tilde{v} \\ \tilde{z}^i \end{bmatrix}^T \begin{bmatrix} \tilde{Q} & \mathbf{0} & \mathbf{0} \\ \mathbf{0} & \tilde{R} & \mathbf{0} \\ \mathbf{0} & \mathbf{0} & \tilde{S} \end{bmatrix} \begin{bmatrix} \tilde{x}^i \\ \tilde{v} \\ \tilde{z}^i \end{bmatrix}, \ i = \underline{d}, \cdots, \overline{d} \tag{22}$$

$$\begin{bmatrix} \tilde{\gamma}_{\min} \\ \tilde{\xi}_{\min} \end{bmatrix} \leq \begin{bmatrix} \tilde{x}^i \\ \tilde{z}^i \end{bmatrix} \leq \begin{bmatrix} \tilde{\gamma}_{\max} \\ \tilde{\xi}_{\max} \end{bmatrix}, \ i = \underline{d}, \cdots, \overline{d} \tag{23}$$

$$\tilde{\delta}_{\min} \leq \tilde{v} \leq \tilde{\delta}_{\max} \tag{24}$$

As Proposition 1 is an SOCP problem (Boyd & Vandenberghe, 2004), its global optimum is easily solved by using some software, e.g. (Sturm, 1999).

Thus, if measured turbulence data have no measurement errors then the addressed problem, i.e. Problem 1, is solved by virtue of Proposition 1 without introducing any conservatism (see Remark 2).

Remark 7. *If Proposition 1 is solved, then the state is bounded by $\gamma_{\min}$ and $\gamma_{\max}$; that is, the boundedness of the state is assured.*

3.2 Measurement error case

Let us suppose that the real turbulence w_{k+j} cannot be measured and the measured turbulence $w_{k+j|k}$ satisfies (13).

First conduct full rank decompositions for matrices $\tilde{Q}$, $\tilde{R}$, and $\tilde{S}$

$$\tilde{Q} = \hat{Q}\hat{Q}^T, \tilde{R} = \hat{R}\hat{R}^T, \tilde{S} = \hat{S}\hat{S}^T.$$

Then, inequality (22) is equivalently transformed to the following inequality by applying the Schur complement (Boyd & Vandenberghe, 2004).

$$
\begin{bmatrix}
q & (\tilde{x}^i)^T \hat{Q} & \tilde{v}^T \hat{R} & (\tilde{z}^i)^T \hat{S} \\
\hat{Q}^T \tilde{x}^i & \mathbf{I} & \mathbf{0} & \mathbf{0} \\
\hat{R}^T \tilde{v} & \mathbf{0} & \mathbf{I} & \mathbf{0} \\
\hat{S}^T \tilde{z}^i & \mathbf{0} & \mathbf{0} & \mathbf{I}
\end{bmatrix} \geq 0
\tag{25}
$$

If some of matrices $\tilde{Q}, \tilde{R}, \tilde{S}$ are set zero matrices, then the corresponding rows and columns in (25) are ignored.

The state $\hat{x}^i_{k+N|k}$ and the performance output $z^i_{k+N-1|k}$ are respectively described as in (26) and (27).

$$
\hat{x}^i_{k+N|k} = (\hat{A}^i)^N \hat{x}^i_{k|k} + \left[(\hat{A}^i)^{N-1}\hat{B}^i_1 \ \cdots \ \hat{A}^i \hat{B}^i_1 \ \hat{B}^i_1\right] \tilde{w} + \left[(\hat{A}^i)^{N-1}\hat{B}^i_2 \ \cdots \ \hat{A}^i \hat{B}^i_2 \ \hat{B}^i_2\right] \tilde{v}
\tag{26}
$$

$$
z^i_{k+N-1|k} = \hat{C}^i (\hat{A}^i)^{N-1} \hat{x}^i_{k|k} + \left[\hat{C}^i(\hat{A}^i)^{N-2}\hat{B}^i_1 \ \cdots \ \hat{C}^i \hat{B}^i_1 \ \hat{D}^i_1\right] \tilde{w} + \left[\hat{C}^i(\hat{A}^i)^{N-2}\hat{B}^i_2 \ \cdots \ \hat{C}^i \hat{B}^i_2 \ \hat{D}^i_2\right] \tilde{v}
\tag{27}
$$

Note that both $\hat{x}^i_{k+N|k}$ and $z^i_{k+N-1|k}$ are affine with respect to each element of Δ_w, because $\tilde{w}$ is affine with respect to each element of Δ_w. Similarly, $\hat{x}^i_{k+m|k}$ $(m = 1, \cdots, N-1)$ and $z^i_{k+m|k}$ $(m = 0, \cdots, N-2)$ are also affine with respect to each element of Δ_w. Considering these and that (25) is affine with respect to $\tilde{x}^i$ and $\tilde{z}^i$, checking whether or not (25) holds for all possible Δ_w is equivalent to checking the feasibility at all vertices of Δ_w.

Now let Φ be defined as the set composed of all the vertices of Δ_w; that is,

$$
\Phi = \left\{ p = [p_1 \ \cdots \ p_{n_w}]^T \in \mathcal{R}^{n_w} : p_i = \pm 1, \ i = 1, \cdots, n_w \right\}.
\tag{28}
$$

The number of the elements belonging to Φ is 2^{n_w}.

Under these preliminaries, the following proposition, which is equivalent to solving Problem 2, is directly obtained.

Proposition 2. *Find $\tilde{v}$ which minimizes q subject to (22), (23) and (24) for all $\Delta_w \in \Phi$.*

Similarly to Proposition 1, as Proposition 2 is also an SOCP problem, its global optimum is easily obtained with the aid of some software, e.g. (Sturm, 1999).

Thus, if the measured turbulence data have measurement errors expressed as $X_j \Delta_w$ and satisfy (13) for the real turbulence, then the addressed problem, i.e. Problem 1, is solved by virtue of Proposition 2 without introducing any conservatism (see Remarks 2 and 5).

Similarly to Remark 7 for Problem 1, if Problem 2 is solved, then the state is bounded by $\gamma_{\min}$ and $\gamma_{\max}$.

Remark 8. *The increases of the numbers N, n_w and i lead to a huge numerical complexity for solving Proposition 2. Thus, obtaining the delay time bounds precisely is very important to reduce i. On the other hand, in general, n_w cannot be reduced, because this number represents the number of channels of turbulence input. The remaining number N has a great impact on controller performance, which will be shown in the next section with numerical simulation results.*

4. Numerical example

Several numerical examples are shown to demonstrate that the proposed method works well for GA problem under the condition that there exist bounded uncertain delays at the control input and the measurement errors in *a priori* measured turbulence data.

4.1 Small aircraft example

Let us first consider the linearized longitudinal aircraft motions of JAXA's research aircraft MuPAL-α (Sato & Satoh, 2008) at an altitude of 1524 [m] and a true air speed of 66.5 [m/s]. This aircraft is based on Dornier Do-228, which is a twin turbo-prop commuter aircraft.

4.1.1 Simulation setting

It is supposed that only the elevator is used for aircraft motion control. The transfer function of its actuator dynamics is modeled as $1/(0.1s + 1)$. Then, the continuous-time system representing the linearized longitudinal motions with the modeled actuator dynamics is given as (1), where the state is $[u_i \ w_i \ q \ \theta \ \delta_e]^T$, the turbulence is w_g, the control input is δ_{e_c}, and the performance output is Δa_z. Here, u_i [m/s], w_i [m/s], q [rad/s], θ [rad], δ_e [rad], w_g [m/s], δ_{e_c} [rad/s] and Δa_z [m/s²] respectively denote inertial forward-backward velocity in body axes, inertial vertical velocity in body axes, pitch rate, pitch angle, elevator deflection, vertical turbulence in inertial axes, elevator command, and vertical acceleration deviation in inertial axes.

After the discretization of (1) with sampling period T_s [s] being set as 0.1, the discrete-time system (5) is given as (29).

$$
\begin{bmatrix} A & B_1 & B_2 \\ C & D_1 & D_2 \end{bmatrix}
$$
$$
= \left[
\begin{array}{ccccc|cc}
0.99799 & 0.018181 & -0.54564 & -0.97647 & 0.11430 & 0.018289 & 0.048318 \\
-0.014894 & 0.87690 & 5.5175 & -0.076329 & -1.1947 & -0.12116 & -0.50903 \\
7.7845 \times 10^{-4} & -5.9106 \times 10^{-3} & 0.80765 & 5.0506 \times 10^{-4} & -0.23770 & -5.9576 \times 10^{-3} & -0.14529 \\
3.9313 \times 10^{-5} & -3.1213 \times 10^{-4} & 0.090399 & 1.0000 & -0.014529 & -3.1444 \times 10^{-4} & -5.3277 \times 10^{-3} \\
0 & 0 & 0 & 0 & 0.36788 & 0 & 0.63212 \\
\hline
-0.18089 & -1.1043 & -1.6792 & 5.8933 \times 10^{-3} & -4.9603 & -1.0825 & 0
\end{array}
\right] \quad (29)
$$

The bounded time-invariant uncertain delay T_d [s] for elevator command is supposed to be in the interval $[0.1, 0.4]$. As the delay time is set as $[0.1, 0.4]$ and the sampling period T_s is 0.1, $\underline{d}$ and $\overline{d}$ are respectively given as 1 and 4. Next the state-space matrices of P_u^i $(i = 1, \cdots, 4)$ are calculated. (The state-space matrices are omitted for space problem.) The augmented state $\hat{x}_k^i$ is given as $\left[u_i \ w_i \ q \ \theta \ \delta_e \ \delta_{e_c(-4)} \ \delta_{e_c(-3)} \ \delta_{e_c(-2)} \ \delta_{e_c(-1)} \right]^T$, where $\delta_{e_c(-l)}$ denotes the elevator command created at l step before. The objective is to obtain the elevator input command,

$\delta_{e_c(0)}$, which minimizes the effect of vertical turbulence to vertical acceleration for all possible delays.

The constraints for the augmented state $\hat{x}_k^i$ and the control input command deviation are given as follows:

$$\gamma_{\max} = \begin{bmatrix} 10 & 10 & \frac{10\pi}{180} & \frac{10\pi}{180} & \frac{5\pi}{180} \times \mathbf{1}_5 \end{bmatrix}^T, \ \gamma_{\min} = -\gamma_{\max},$$
$$\delta_{\max} = \frac{\pi}{180}, \ \delta_{\min} = -\delta_{\max}.$$

This means that the rate limit of elevator command is set as $\pm 10 \, [\text{deg/s}]$. The constraints for performance output $\zeta_{\min}$ and $\zeta_{\max}$ are respectively set as $-\infty$ and ∞; that is, performance output has no constraints.

Matrices Q and S in (16) are set as $Q = 0_9$ and $S = 1$ respectively. Matrix R will be set later. The turbulence w_g is supposed to be given as

$$w_g(t) = \sin(\omega t), \tag{30}$$

where t denotes the simulation time starting from 0, and ω, which will be set later, denotes the frequency of the turbulence.

4.1.2 Simulation results without measurement errors in turbulence data

Let us first show the results of simulations in which turbulence is supposed to be exactly measured.

Numerical simulations using continuous-time system (1) composed of MuPAL-α's linearized longitudinal motions and the first-order elevator actuator model, and the proposed MPC in which Proposition 1 is solved on line are carried out for 20 [s]. In the simulations, various constant delay steps at the control input $\hat{t}_d$, various constant turbulence frequencies ω [rad/s], various constant weighting matrices R, and various constant receding horizon step numbers N are used from the following sets:

$$\begin{aligned} \hat{t}_d &\in \{1, \ 2, \ 3, \ 4\}, \\ \omega &\in \{0.1, \ 0.5, \ 1.0, \ 5.0, \ 7.0, \ 8.0, \ 10.0\}, \\ R &\in \left\{10^{-1}, \ 10^0, \ 10^1, \ 10^2, \ 10^3, \ 10^4\right\}, \\ N &\in \{10, \ 20, \ 30, \ 40, \ 50\}. \end{aligned} \tag{31}$$

For comparison, the following scenarios are simultaneously carried out.

Scenario A: MPC in which Proposition 1 is solved online is applied,

Scenario B: no control is applied,

Scenario C: MPC in which Proposition 1 is solved online but with the measured turbulence data being set as zeros, i.e. MPC without prior turbulence data, is applied.

Fig. 3 shows the performance comparison for scenarios A, B and C. In this figure, J_A, J_B and J_C denote the following performance indices for the corresponding scenarios, which are obtained from the simulations:

$$\max_{\hat{t}_d \in \{1, \ 2, \ 3, \ 4\}} \int_0^{20} |\Delta a_z|^2 dt. \tag{32}$$

For comparison, mesh planes at $J_A/J_B = 1$ and $J_A/J_C = 1$ are drawn. $J_A/J_B < 1$ means that gust alleviation is effectively achieved by the proposed method, and $J_A/J_C < 1$ means that the *a priori* measured turbulence data are useful for the improvement of GA performance. The following are concluded from Fig. 3.

- It is very difficult for MuPAL-α to suppress high frequency turbulence effect, such as, over 8 [rad/s].
- MuPAL-α has no need to measure turbulence *a priori* for more than 20 steps. In other words, it is sufficient for MuPAL-α to measure turbulence for 20 steps ahead.
- Using an appropriately chosen R (e.g. $R = 10^2$), the proposed GA flight controller in which Proposition 1 is solved online improves GA performance for low and middle frequency turbulence, such as, below 5 [rad/s].

The first item is reasonable because aircraft motion model has a direct term from the vertical turbulence to the vertical acceleration and it is supposed that there exists uncertain delay at its control input. The second item is interesting, because there is a limit for the improvement of GA performance even when *a priori* measured turbulence data are available.

For reference, several time histories with $R = 10^2$ and $N = 20$ are shown in Fig. 4. For space problem, only actual elevator deflection command (δ_{e_c}) and its created command by flight computer ($\delta_{e_c(0)}$), and performance output are shown. δ_{e_c} and $\delta_{e_c(0)}$ almost overlap in some cases. These figures illustrate the usefulness of the *a priori* measured turbulence data.

4.1.3 Simulation results with measurement errors in turbulence data

Let us next show the results of simulations in which measured turbulence data have measurement errors.

Numerical simulations using continuous-time system (1) composed of MuPAL-α's linearized longitudinal motions and the first-order elevator actuator model, and the proposed MPC in which Proposition 2 is solved on line are carried out for 20 [s]. In the simulations, various constant delay steps at the control input $\hat{t}_d$, various constant turbulence frequencies ω [rad/s], various constant weighting matrices R, and various constant receding horizon step numbers N are used from the following sets:

$$\begin{aligned}
&\hat{t}_d \in \{1,\ 2,\ 3,\ 4\}\,,\\
&\omega \in \{0.1,\ 0.5,\ 1.0,\ 3.0,\ 4.0,\ 5.0,\ 6.0,\ 7.0\}\,,\\
&R \in \{10^1,\ 10^2,\ 10^3,\ 10^4,\ 10^5\}\,,\\
&N \in \{10,\ 12,\ 14,\ 16,\ 18,\ 20,\ 22,\ 24\}\,.
\end{aligned} \tag{33}$$

Matrices X_j in the measurement error are set as

$$X_j = 0.2 + 0.1 \times (66.5/100 \times T_s)\, j. \tag{34}$$

This means that the measurement error for w_g is composed of a constant bias error 0.2 [m/s] and a measurement error which is proportional to distance, the latter has 0.1 [m/s] measurement error at 100 [m] ahead.

Three possibilities are considered in the simulations; that is, (i) the real turbulence is the same as the measured turbulence, i.e. $w_{k+j} = w_{k+j|k}$, (ii) the real turbulence is the upper bound of the supposed turbulence, i.e. $w_{k+j} = w_{k+j|k} + X_j$ using (34), and (iii) the real turbulence is the lower bound of the supposed turbulence, i.e. $w_{k+j} = w_{k+j|k} - X_j$ using (34).

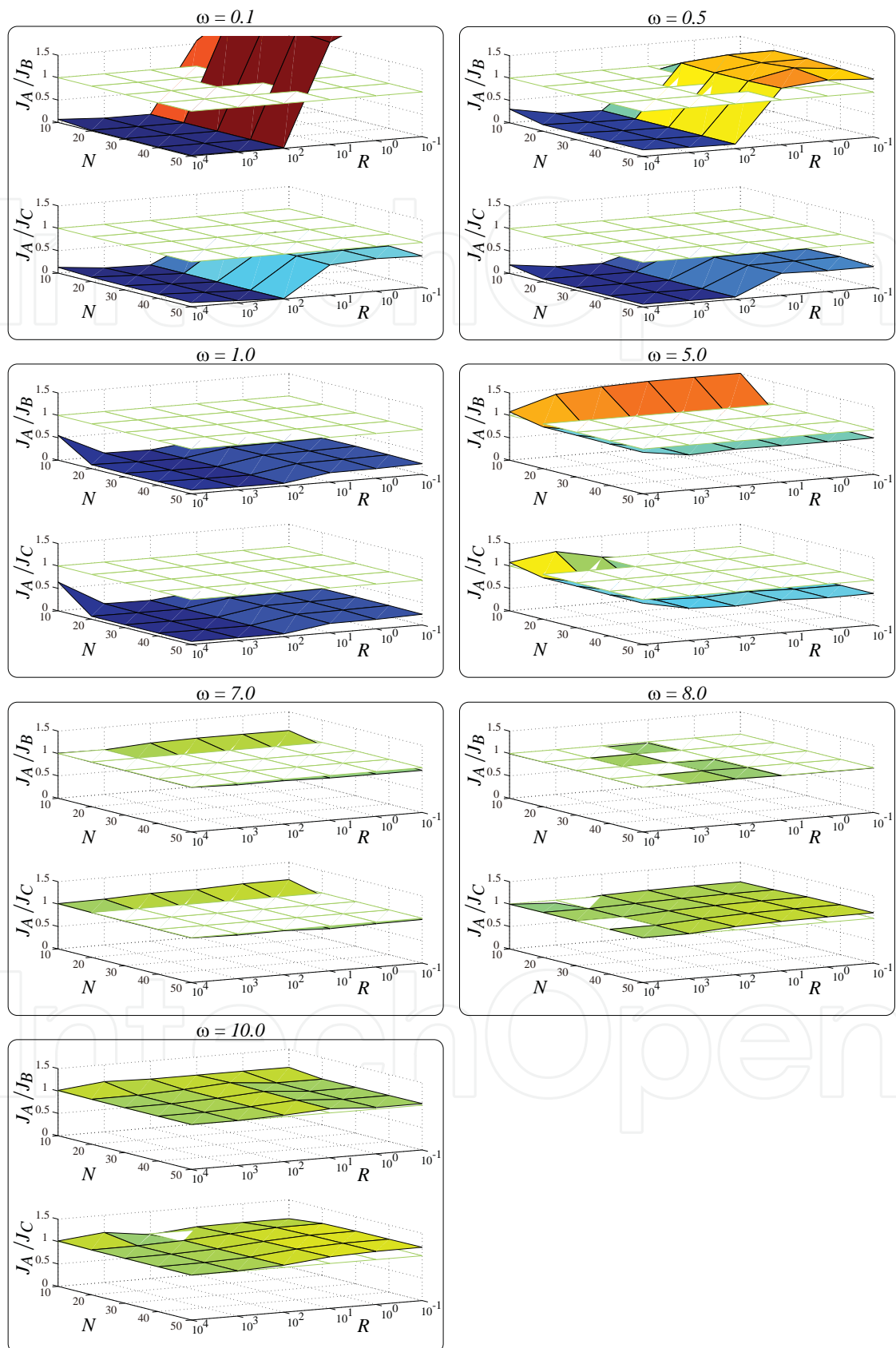For comparison, the following scenarios are simultaneously carried out.

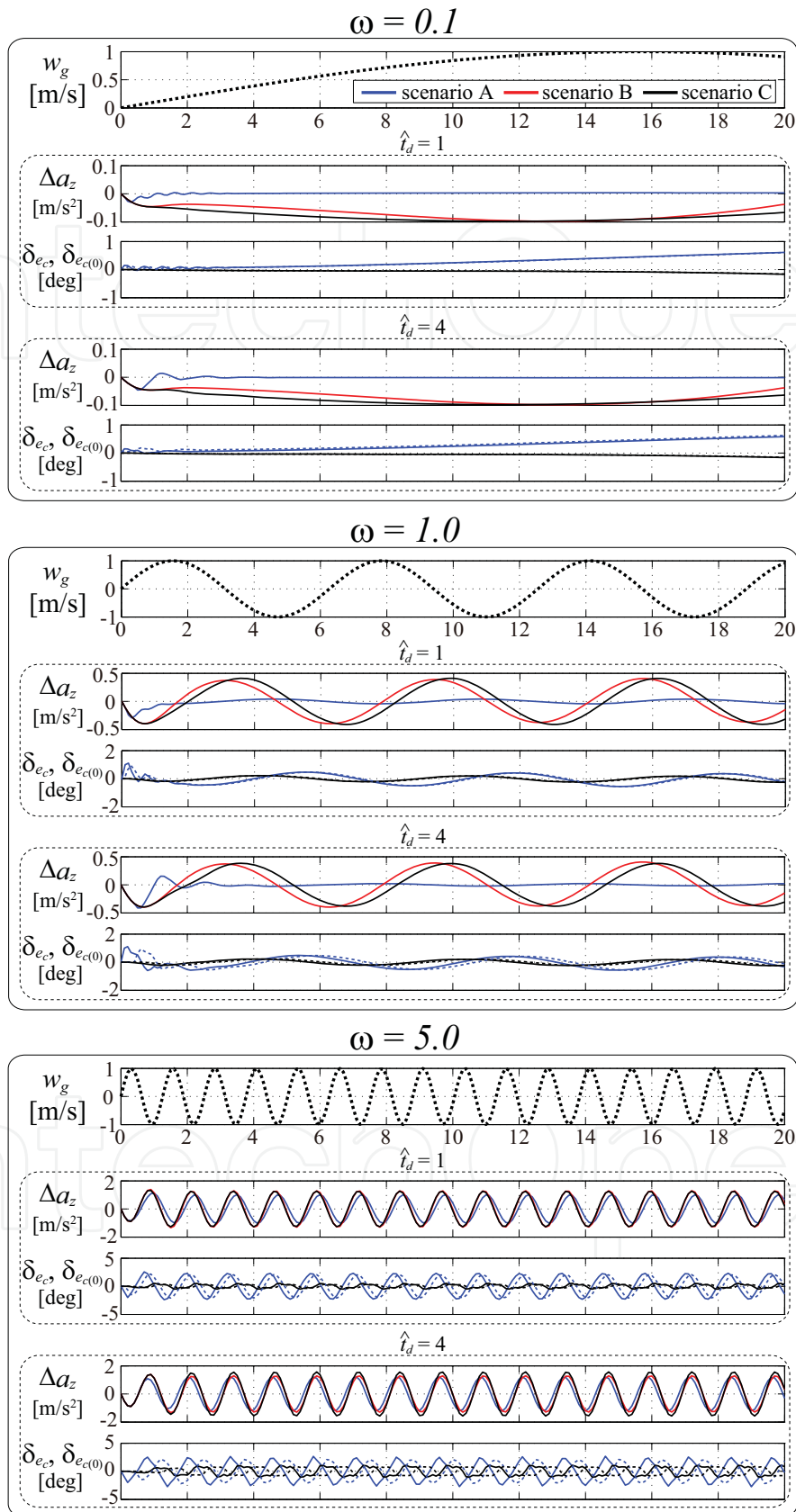Fig. 3. GA performance comparison for MuPAL-α under no measurement errors in turbulence data

Fig. 4. Time histories under no measurement errors in turbulence data with $R = 10^2$ and $N = 20$ (δ_{e_c} is shown as dotted lines and $\delta_{e_{c(0)}}$ is shown as solid lines)

Scenario A: MPC in which Proposition 2 is solved online is applied,

Scenario B: no control is applied,

Scenario C: MPC in which Proposition 2 is solved online but with the measured turbulence data being set as zeros, i.e. MPC without prior turbulence data, is applied.

Fig. 5 shows the performance comparison for scenarios A, B and C. In this figure, J_A, J_B and J_C denote the following performance indices for the corresponding scenarios, which are obtained from the simulations:

$$\max_{w_{k+j}=\left\{w_{k+j|k},\, w_{k+j|k}\pm X_j\right\}} \max_{\hat{t}_d \in \{1,\, 2,\, 3,\, 4\}} \int_0^{20} |\Delta a_z|^2 dt. \tag{35}$$

For comparison, mesh planes at $J_A/J_B = 1$ and $J_A/J_C = 1$ are drawn.
The following are concluded from Fig. 5.

- For turbulence, whose frequencies are no more than $0.5\,[\text{rad}/\text{s}]$, GA performance using the proposed method is larger than the uncontrolled case.

- For turbulence, whose frequencies are more than $6\,[\text{rad}/\text{s}]$, vertical acceleration is hardly reduced even if prior turbulence data are obtained.

- It is sufficient for MuPAL-α to measure turbulence for 20 steps ahead.

- Using an appropriately chosen R (e.g. $R = 10^3$), the proposed GA flight controller in which Proposition 2 is solved online improves GA performance for middle frequency turbulence, such as, $1 \sim 5\,[\text{rad}/\text{s}]$.

The first item does not hold true for no measurement error case (see also Fig. 3). Thus, GA performance deterioration for low frequency turbulence is caused by the measurement errors in the measured turbulence data. The second item is reasonable for considering that it is difficult to suppress turbulence effect on aircraft motions caused by high frequency turbulence even when the turbulence is exactly measured (see also Fig. 3). The fourth item illustrates that the *a priori* measured turbulence data improve GA performance even when there exist measurement errors in the measured turbulence data.

For reference, several time histories with $R = 10^3$, $N = 18$ and $\hat{t}_d = 4$ are shown in Fig. 6. For space problem, only actual elevator deflection command (δ_{e_c}) and its created command by flight computer ($\delta_{e_c(0)}$), and performance output are shown. These figures illustrate the usefulness of the *a priori* measured turbulence data for middle frequency turbulence (e.g. 1.0 and $5.0\,[\text{rad}/\text{s}]$). However, as the top figure in Fig. 6 indicates, measurement errors in turbulence data deteriorate GA performance; that is, if the real turbulence is smaller than the measured one, i.e. the case for $w_{k+j} = w_{k+j|k} - X_j$, then the proposed MPC produces surplus elevator deflections and this causes extra downward accelerations. The converse, i.e. the case for $w_{k+j} = w_{k+j|k} + X_j$, also holds true. Thus, it is very important for achieving good GA performance to measure turbulence exactly.

To evaluate the impact of the rate limit for elevator command on GA performance, the same simulations but with only $\delta_{\max}$ and $\delta_{\min}$ being doubled, i.e. $\delta_{\max} = 2\frac{\pi}{180}$ and $\delta_{\min} = -2\frac{\pi}{180}$, are carried out. The results for (35) are shown in Fig. 7.
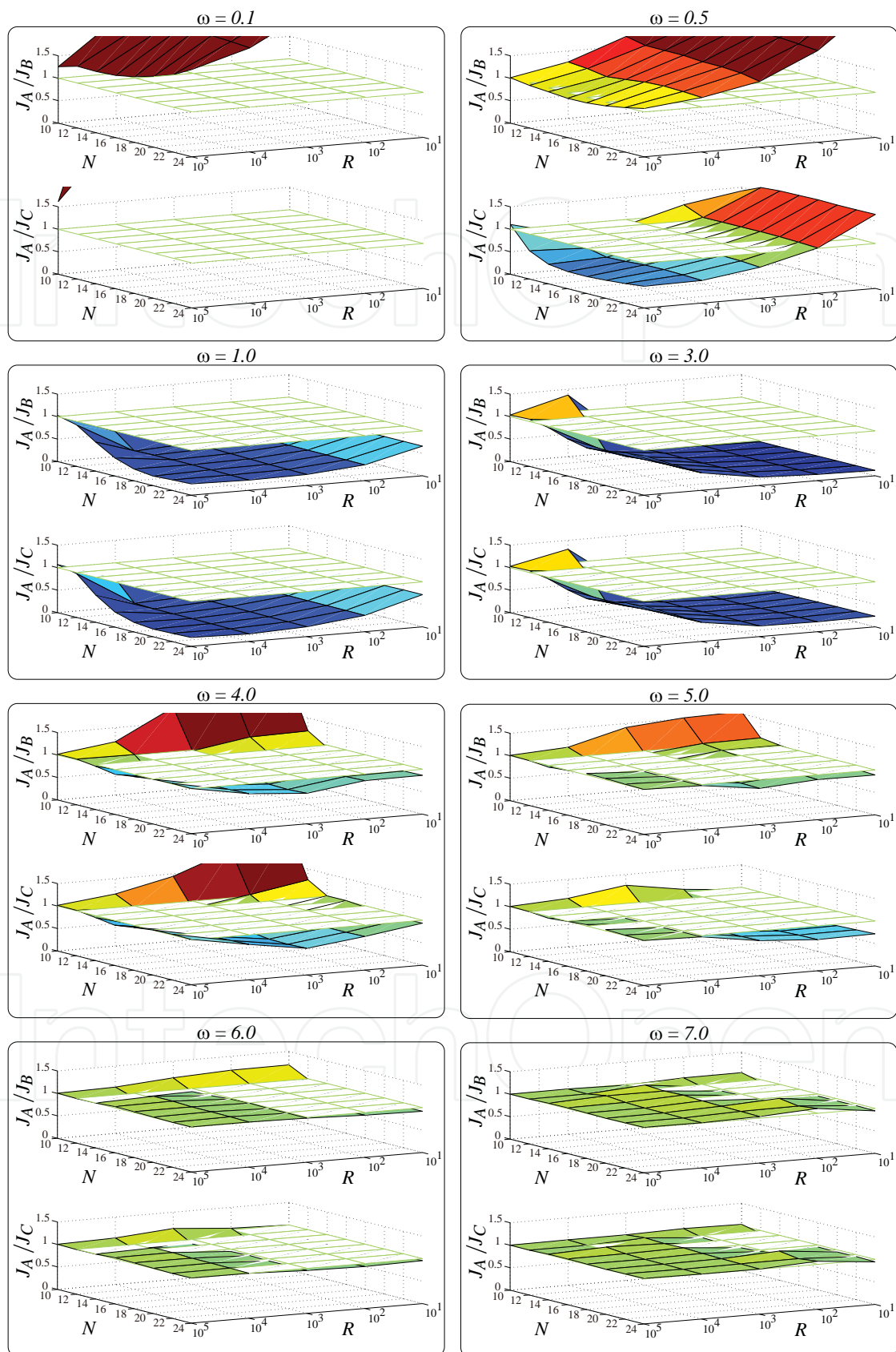Comparison between Figs. 5 and 7 concludes the following.

Fig. 5. GA performance comparison for MuPAL-*α* under measurement errors in turbulence data
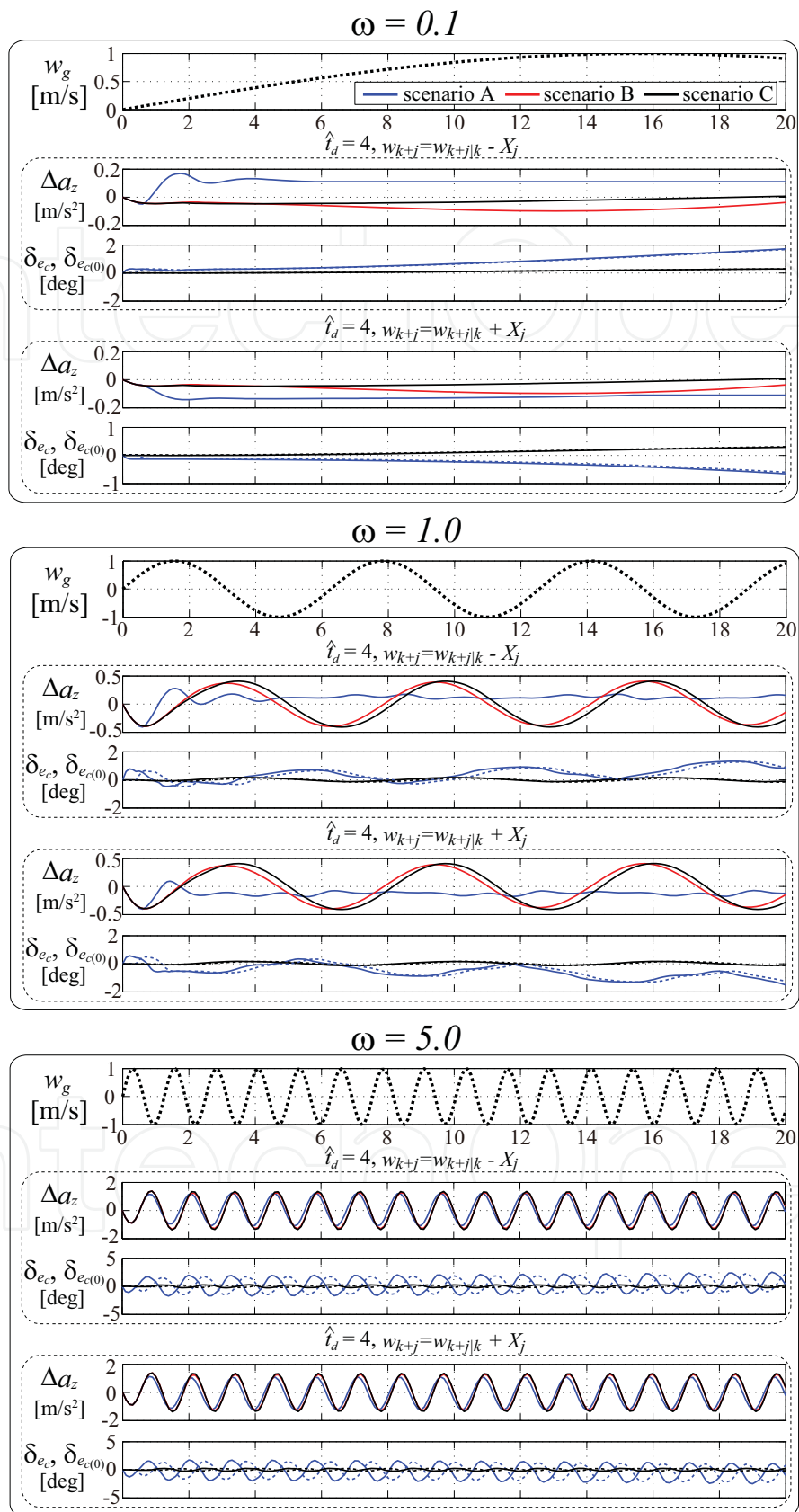
Fig. 6. Time histories under measurement errors in turbulence data with $R = 10^3$ and $N = 18$ (δ_{e_c} is shown as dotted lines and $\delta_{e_c(0)}$ is shown as solid lines)
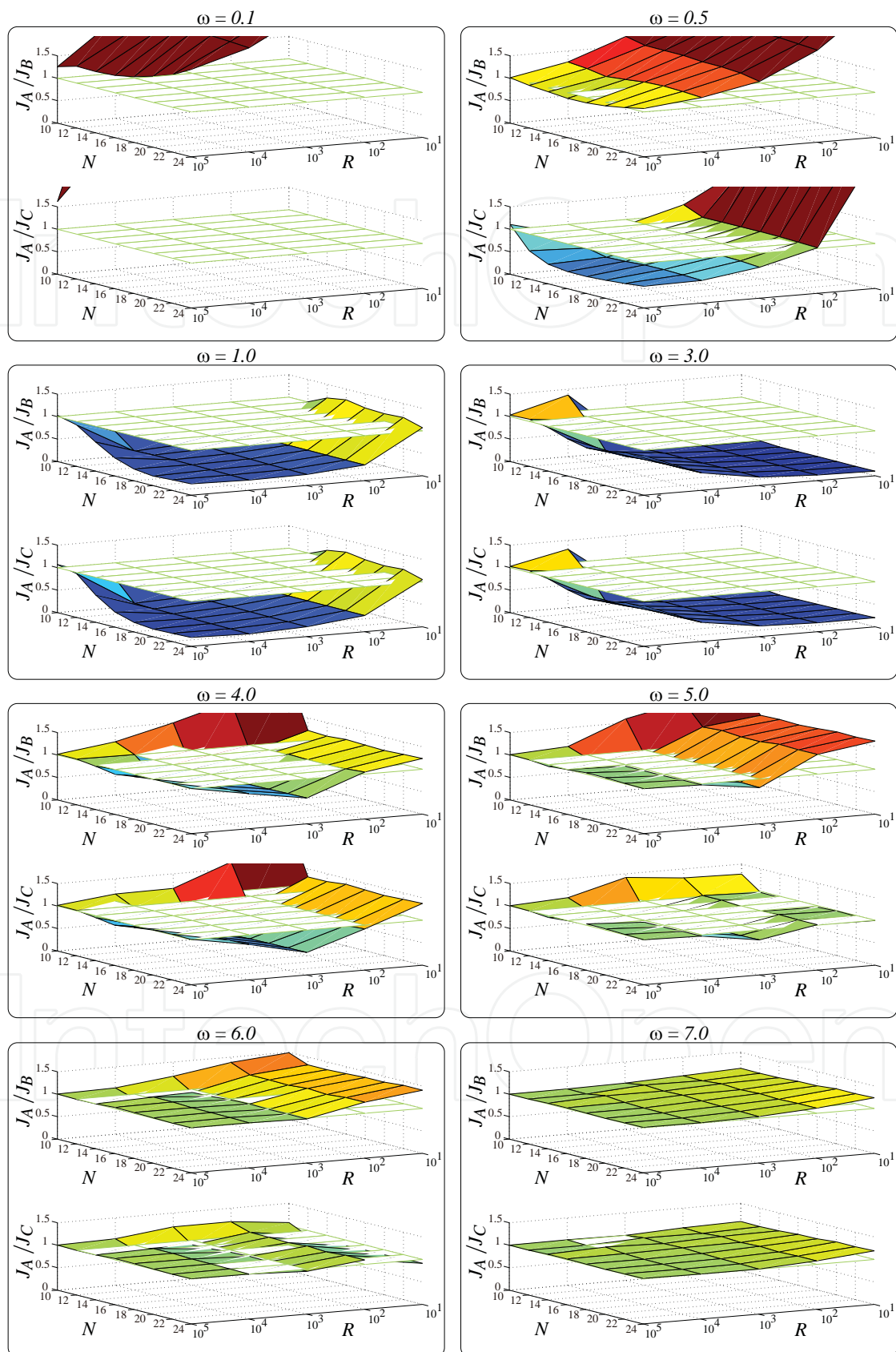
Fig. 7. GA performance comparison for MuPAL-*α* with relaxed rate limit for elevator command under measurement errors in turbulence data

ω [rad/s]	R	N	PT7400	P650
0.1	10^1	10	$0.30 - 0.52(0.38)$	$0.88 - 1.45(1.18)$
		24	$0.47 - 1.36(0.74)$	$1.78 - 3.94(2.52)$
	10^5	10	$0.27 - 0.49(0.34)$	$0.84 - 1.25(1.03)$
		24	$0.40 - 1.00(0.59)$	$1.14 - 2.78(2.01)$
1.0	10^1	10	$0.29 - 0.53(0.37)$	$0.97 - 1.48(1.18)$
		24	$0.45 - 3.62(0.76)$	$1.64 - 3.94(2.52)$
	10^5	10	$0.26 - 0.43(0.32)$	$0.80 - 1.44(0.99)$
		24	$0.39 - 1.02(0.59)$	$1.36 - 2.64(1.98)$
6.0	10^1	10	$0.30 - 0.53(0.38)$	$0.77 - 1.41(1.17)$
		24	$0.51 - 0.96(0.69)$	$2.08 - 2.88(2.38)$
	10^5	10	$0.26 - 0.51(0.34)$	$0.81 - 1.28(1.00)$
		24	$0.43 - 0.82(0.58)$	$1.77 - 2.50(2.04)$

Table 1. CPU time [s] (max − min (average))

- The rate limit for elevator command does not have so large impact on GA performance except for the cases using small R.

This fact is reasonable because it is difficult to suppress high frequency turbulence effect even when there are no measurement errors in the turbulence data (see Fig. 3), and if R is set relatively large, e.g. $R = 10^3$, then MuPAL-α has no need to use high rate elevator commands for suppressing middle frequency turbulence effect, such as, 1.0 [rad/s] (see Fig. 6). However, if R is set small then the proposed GA flight controller allows high rate elevator commands, which lead to severe oscillatory accelerations. Thus, GA performance deteriorates.

Finally, CPU time to solve Proposition 2 is shown in Table 1. The simulation setting is the same as for obtaining the results in Fig. 5. The simulations are conducted with Matlab® using SeDuMi (Sturm, 1999) along with a parser YALMIP (Löfberg, 2004) with a PC (Dell Precision T7400, Xeon®3.4 GHz, 32 GB RAM; PT7400) and a PC (Dell Precision 650, Xeon®3.2 GHz, 2 GB RAM; P650). Although CPU time with PT7400 is just about 30 % of P650, at the present moment, solving Proposition 2 online is impossible with these PCs even when N is set as 10. Thus, the reduction of numerical complexity for solving Proposition 2 is to be investigated.

4.2 Large aircraft example
Let us next consider the linearized longitudinal aircraft motions of large aircraft Boeing 747 (B747) (Heffley & Jewell, 1972) at an altitude of 12192 [m] and a true air speed of 236 [m/s].

4.2.1 Simulation setting
Similarly to MuPAL-α, it is supposed that only the elevator is used for aircraft motion control. The transfer function of its actuator dynamics is also supposed to be modeled as $1/(0.1s + 1)$. Then, the continuous-time system representing the linearized longitudinal motions with the modeled actuator dynamics is given as (1), where the state, the turbulence, the control input, and the performance output are the same as MuPAL-α.

After the discretization of (1) with sampling period T_s [s] being set as 0.1 using a zero-order hold, the discrete-time system (5) is given as (36).

$$
\begin{bmatrix} A & B_1 & B_2 \\ \hline C & D_1 & D_2 \end{bmatrix}
$$

$$
= \left[\begin{array}{ccccc}
0.99965 & 4.1350 \times 10^{-3} & -1.8544 & -0.97754 & 0.10639 \\
-5.6762 \times 10^{-3} & 0.96481 & 22.643 & -0.074565 & -1.3157 \\
6.5386 \times 10^{-5} & -3.1960 \times 10^{-4} & 0.95423 & 1.0244 \times 10^{-5} & -0.071212 \\
3.2771 \times 10^{-6} & -1.6194 \times 10^{-5} & 0.097759 & 1.0000 & -4.1894 \times 10^{-3} \\
0 & 0 & 0 & 0 & 0.36788 \\
\hline
-0.065004 & -0.32122 & -5.3617 \times 10^{-3} & -5.2561 \times 10^{-3} & -5.5100
\end{array} \right.
$$

$$
\left. \begin{array}{c|c}
4.1498 \times 10^{-3} & 0.044513 \\
-0.034623 & -0.55260 \\
-3.2381 \times 10^{-4} & -0.041894 \\
-1.6405 \times 10^{-5} & -1.5116 \times 10^{-3} \\
0 & 0.63212 \\
\hline
-0.31497 & 0
\end{array} \right]
$$

(36)

The delay T_d for elevator command, the constraints for the augmented state, the control input command deviation and the performance output, matrices Q and S in (16), the turbulence, and the measurement errors are all set the same as for MuPAL-α.

4.2.2 Simulation results

The same numerical simulations in section 4.1.3 but the aircraft motion model being replaced by the B747 model are carried out for the following parameter setting.

$$
\begin{aligned}
\hat{t}_d &\in \{1, 2, 3, 4\}, \\
\omega &\in \{0.1, 0.5, 1.0, 3.0, 4.0, 5.0, 6.0\}, \\
R &\in \{10^{-1}, 10^0, 10^1, 10^2, 10^3, 10^4, 10^5, 10^6, 10^7\}, \\
N &\in \{10, 12, 14, 16, 18, 20, 22, 24\}.
\end{aligned}
$$

(37)

Fig. 8 shows the performance comparison for scenarios A, B and C. In this figure, J_A, J_B and J_C are similarly calculated as in Fig. 5.

The following are concluded from Fig. 8.

- For turbulence, whose frequencies are no more than 0.1 [rad/s], GA performance using the proposed method is larger than the uncontrolled case.

- For turbulence, whose frequencies are more than 5 [rad/s], vertical acceleration is hardly reduced even if prior turbulence data are obtained.

- It is sufficient for B747 to measure turbulence for 20 steps ahead.

- Using an appropriately chosen R (e.g. $R = 10^3$), the proposed GA flight controller in which Proposition 2 is solved online improves GA performance for middle frequency turbulence, such as, $0.5 \sim 4$ [rad/s].

Differently from MuPAL-α, low frequency turbulence effect to B747, e.g. 0.5 [rad/s], can be reduced by the proposed GA controller; however, middle frequency turbulence effect, e.g. 5 [rad/s], cannot be reduced. The third item is interesting in a sense that the step number
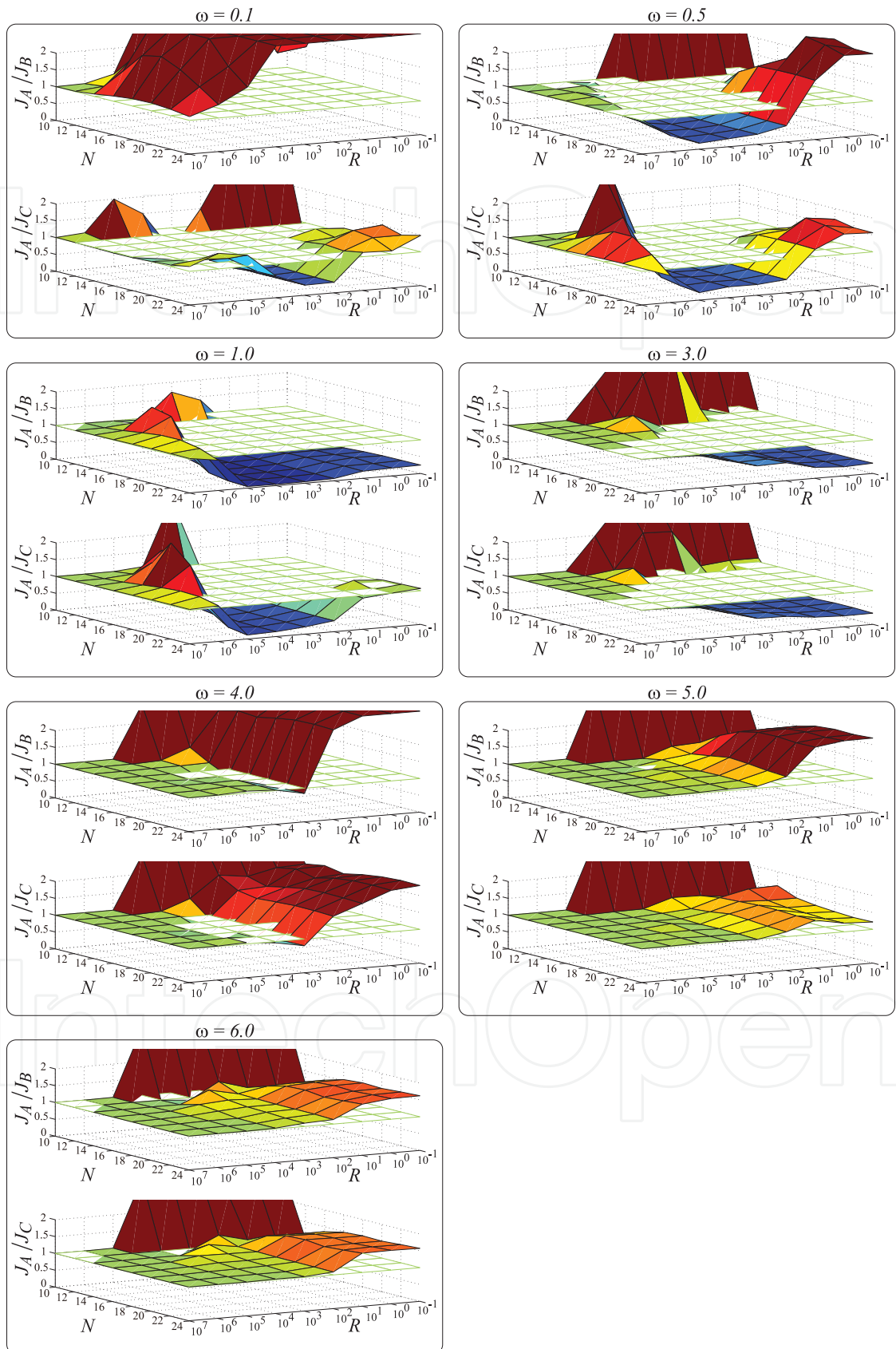
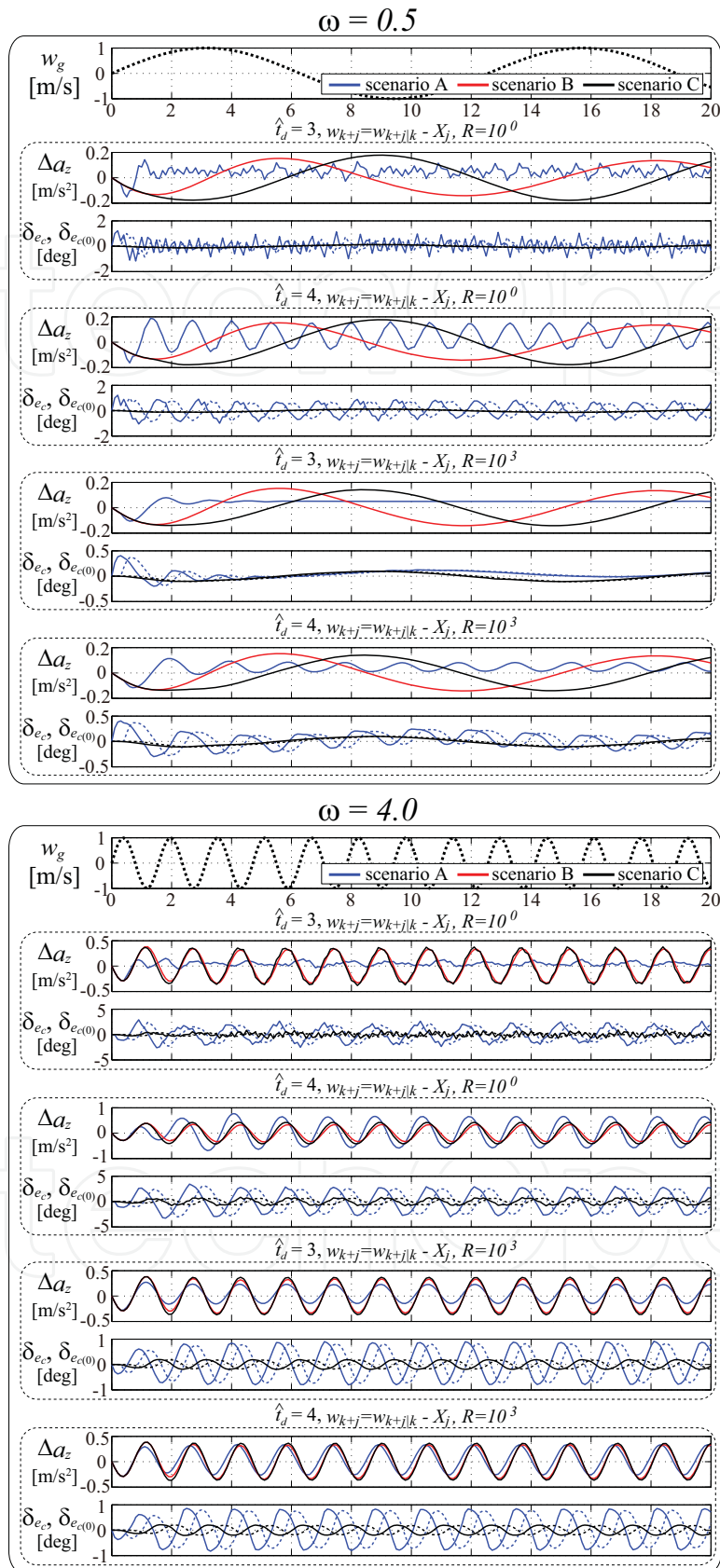Fig. 8. GA performance comparison for B747 under measurement errors in turbulence data

Fig. 9. Time histories for B747 under measurement errors in turbulence data with $N = 18$ (δ_{e_c} is shown as dotted lines and $\delta_{e_c(0)}$ is shown as solid lines)

for turbulence measurement does not depend on aircraft models. However, it is not sure that this fact indeed holds for other aircraft, which is to be investigated.

For reference, several time histories with $N = 18$, $R = 10^0$ or 10^3, and $\hat{t}_d = 3$ or 4 are shown in Fig. 9. For space problem, only actual elevator deflection command (δ_{e_c}) and its created command by flight computer ($\delta_{e_c(0)}$), and performance output are shown. These figures confirm that small R, i.e. $R = 10^0$, allows large elevator deviation commands and this consequently leads to severely oscillatory vertical accelerations. However, the proposed controller with an appropriately chosen R, i.e. $R = 10^3$, well suppresses turbulence effect on aircraft motions.

5. Conclusions

This paper tackles the design problem of Gust Alleviation (GA) flight controllers exploiting *a priori* measured turbulence data for suppressing aircraft motions driven by turbulence. For this problem, a robust Model Predictive Control (MPC) considering the plant uncertainties and the measurement errors in the turbulence data is proposed. In the usual setting, MPC for uncertain plant requires to solve an optimization problem with infinitely many conditions if conservatism is avoided. However, it is shown that if the plant uncertainties are represented as the bounded time-invariant uncertain delays at the control input, then the associated problem for the robust MPC is equivalently transformed to an optimization problem for finitely many plant models, which consequently means that the optimization problem has finitely many conditions.

In our problem setting, the measurement errors in the *a priori* measured turbulence data are represented as affine with respect to a constant uncertain vector, whose elements are all bounded. Using this property, it is shown that it is necessary and sufficient to evaluate the performance index in MPC at the maxima and minima of the uncertain vector. This consequently means that the robust MPC has finitely many conditions even when the measurement errors are considered.

Several numerical examples illustrate that the proposed GA flight controller with appropriately chosen controller parameters effectively suppresses turbulence effect on aircraft motions, and reveal that it is very difficult to suppress high frequency turbulence effect even when the *a priori* measured turbulence data are exploited.

To guarantee the feasibility of the proposed MPC at every step is an important issue for the implementation of the proposed method to real systems. Thus, this topic is now under investigation.

6. References

Abdelmoula, F. (1999). Design of an open-loop gust alleviation control system for airborne gravimetry, *Aerospace Science and Technology* Vol. 3(No. 6): 379–389.

Ando, T., Kameyama, S. & Hirano, Y. (2008). All-fiber coherent doppler LIDAR technologies at mitsubishi electric corporation, *14th Int. Sympo. for Advancement of Boundary Layer Remote Sensing*.

Badgwell, T. A. (1997). Robust model predictive control of stable linear systems, *Int. J. Control* Vol. 68(No. 4): 797–818.

Bemporad, A. & Morari, M. (1999). *Robustness in Identification and Control*, Springer Verlag, Berlin, chapter Robust Model Predictive Control: A Survey. Lecture Notes in Control and Information Sciences 245.

Botez, R. M., Boustani, I., Vayani, N., Bigras, P. & Wong, T. (2001). Optimal control laws for gust alleviation, *Canadian Aeronautics and Space Journal* Vol. 47(No. 1): 1–6.

Boyd, S. & Vandenberghe, L. (2004). *Convex Optimization*, Cambridge University Press, Cambridge.

Fujita, M., Hatake, K. & Matsumura, F. (1993). Loop shaping based robust control of a magnetic bearing, *IEEE Control Systems Magazine* Vol. 13(No. 4): 57–65.

Heffley, R. K. & Jewell, W. F. (1972). *Aircraft Handling Qualities Data*, National Aeronautics and Space Administration, Washington, D.C.

Hess, R. A. (1971). Optimal stochastic control and aircraft gust alleviation, *Journal of Aircraft* Vol. 8(No. 4): 284–286.

Hess, R. A. (1972). Some results of suboptimal gust alleviation, *Journal of Aircraft* Vol. 9(No. 5): 380–381.

Inokuchi, H., Tanaka, H. & Ando, T. (2009). Development of an onboard doppler lidar for flight safety, *J. Aircraft* Vol. 46(No. 4): 1411–1415.

Jenaro, G., Mirand, P., Raymond, M., Schmitt, N., Pistner, T. & Rehm, W. (2007). Airborne forward looking lidar system, *Int. Forum on Aeroelasticity and Structural Dynamics*. IF-088.

Kothare, M. V., Balakrishnan, V. & Morari, M. (1996). Robust constrained model predictive control using linear matrix inequalities, *Automatica* Vol. 32: 1361–1379.

Kwon, W. H. & Han, S. (2005). *Receding Horizon Control: model predictive control for state models*, Springer-Verlag, London.

Löfberg, J. (2003). *Minimax Approaches to Robust Model Predictive Control*, PhD thesis, Linköping University, Linköping, Sweden.

Löfberg, J. (2004). YALMIP: A toolbox for modeling and optimization in MATLAB, *Proc. the CACSD Conference*, Taipei, Taiwan.
  URL: *http://control.ee.ethz.ch/ joloef/yalmip.php*

Mehra, R. K., Amin, J. N., Hedrick, K. J., Osorio, C. & Gopalasamy, S. (1997). Active suspension using preview information and model predictive control, *Proc. CCA*, pp. 860–865.

Military Specification: Flight Control Systems - Design, Installation and Test of Piloted Aircraft, General Specification For (1975). MIL-F-9490D.

Miyazawa, Y. (1995). Design with multiple-delay-model and multiple-design-point approach, *J. Guidance, Control, and Dynamics* Vol. 18(No. 3): 508–515.

Ohno, M., Yamaguchi, Y., Hata, T., Takahama, M., Miyazawa, Y. & Izumi, T. (1999). Robust flight control law design for an automatic landing flight experiment, *Control Engineering Practice* Vol. 7: 1143–1151.

Phillips, W. H. (1971). *Gust Alleviation*, National Aeronautics and Space Administration, Washington, D.C., pp. 505–553. NASA SP-258.

Rynaski, E. G. (1979a). Gust alleviation - criteria and control laws, AIAA. AIAA Paper 1979-1676.

Rynaski, E. G. (1979b). Gust alleviation using direct turbulence measurements, AIAA. AIAA Paper 1979-1674.

Santo, X. D. & Paim, P. K. (2008). Multi-objective and predictive control - application to the clear air turbulence issues, *AIAA Guidance, Navigation and Control Conference*, AIAA. AIAA Paper 2008-7141.

Sato, M. & Satoh, A. (2008). Simultaneous realization of handling and gust responses: In-flight simulator controller design, *J. Guidance, Control, and Dynamics* Vol. 37(No. 6): 1545–1560.

Schmitt, N. P., Rehm, W., Pistner, T., Zeller, P., Diehl, H. & Navé, P. (2007). The AWIATOR airborne LIDAR turbulence sensor, *Aerospace Science and Technology* Vol. 11: 546–552.

Sturm, J. S. (1999). Using SeDuMi 1.02, a MATLAB toolbox for optimization over symmetric cones, *Optimization Methods and Software* Vols. 11-12: 625–653.

Takaba, K. (2000). Robust servomechanism with preview action for polytopic uncertain systems, *Int. J. Robust and Nonlinear Control* Vol. 10: 101–111.

Tomizuka, M. (1976). Optimum linear preview control with application to vehicle suspension–revisited, *J. Dynamic Systems, Measurement, and Control* Vol. 98(No. 3): 309–315.

Xie, L. & de Souza, C. E. (1992). Robust H_∞ control for linear systems with norm-bounded time-varying uncertainty, *IEEE Trans. Automatic Control* Vol. 37(No. 8): 1188–1191.

Xie, L., Fu, M. & de Souza, C. E. (1992). H_∞ control and quadratic stabilization of systems with parameter uncertainty via output feedback, *IEEE Trans. Automatic Control* Vol. 37(No. 8): 1253–1256.

Zhou, K., Doyle, J. C. & Glover, K. (1996). *Robust and Optimal Control*, Prentice-Hall, Upper Saddle River, NJ.

Advanced Model Predictive Control

Edited by Dr. Tao ZHENG

ISBN 978-953-307-298-2

Hard cover, 418 pages

Publisher InTech

Published online 24, June, 2011

Published in print edition June, 2011

Model Predictive Control (MPC) refers to a class of control algorithms in which a dynamic process model is used to predict and optimize process performance. From lower request of modeling accuracy and robustness to complicated process plants, MPC has been widely accepted in many practical fields. As the guide for researchers and engineers all over the world concerned with the latest developments of MPC, the purpose of "Advanced Model Predictive Control" is to show the readers the recent achievements in this area. The first part of this exciting book will help you comprehend the frontiers in theoretical research of MPC, such as Fast MPC, Nonlinear MPC, Distributed MPC, Multi-Dimensional MPC and Fuzzy-Neural MPC. In the second part, several excellent applications of MPC in modern industry are proposed and efficient commercial software for MPC is introduced. Because of its special industrial origin, we believe that MPC will remain energetic in the future.

How to reference

In order to correctly reference this scholarly work, feel free to copy and paste the following:

Masayuki Sato, Nobuhiro Yokoyama and Atsushi Satoh (2011). Gust Alleviation Control Using Robust MPC, Advanced Model Predictive Control, Dr. Tao ZHENG (Ed.), ISBN: 978-953-307-298-2, InTech, Available from: http://www.intechopen.com/books/advanced-model-predictive-control/gust-alleviation-control-using-robust-mpc

INTECH
open science | open minds